

The structure/function relationship of a dual-substrate ($\beta\alpha$)₈-isomerase

Helena Wright ^a, Lianet Noda-García ^b, Adrián Ochoa-Leyva ^b, David A. Hodgson ^a,
Vilmos Fülöp ^a, Francisco Barona-Gómez ^{b,*}

^a Department of Biological Sciences, University of Warwick, Gibbet Hill Road, Coventry CV4 7AL, UK

^b Departamento de Ingeniería Celular y Biocatálisis, Instituto de Biotecnología, Universidad Nacional Autónoma de México (UNAM),
Av. Universidad 2001, Cuernavaca, C.P. 62210, Mexico

Received 12 October 2007

Available online 29 October 2007

Abstract

Two structures of phosphoribosyl isomerase A (PriA) from *Streptomyces coelicolor*, involved in both histidine and tryptophan biosynthesis, were solved at 1.8 Å resolution. A closed conformer was obtained, which represents the first complete structure of PriA, revealing hitherto unnoticed molecular interactions and the occurrence of conformational changes. Inspection of these conformers, including ligand-docking simulations, allowed identification of residues involved in substrate recognition, chemical catalysis and conformational changes. These predictions were validated by mutagenesis and functional analysis. Arg¹⁹ and Ser⁸¹ were shown to play critical roles within the carboxyl and amino phosphate-binding sites, respectively; the catalytic residues Asp¹¹ and Asp¹³⁰ are responsible for both activities; and Thr¹⁶⁶ and Asp¹⁷¹, which make an unusual contact, are likely to elicit the conformational changes needed for adopting the active site architectures. This represents the first report of the structure/function relationship of this ($\beta\alpha$)₈-isomerase.

© 2007 Elsevier Inc. All rights reserved.

Keywords: ($\beta\alpha$)₈-Barrel; PriA; HisA; TrpF; Co-occurrence of conformers

Most members of the actinomycetes family lack a *trpF* gene, which is involved in the tryptophan biosynthetic pathway. The protein product of *trpF* is the ($\beta\alpha$)₈-enzyme *N*'-(5'-phosphoribosyl)anthranilate (PRA) isomerase (TrpF, EC 5.3.1.24), which converts the aminoaldose PRA into its cognate aminoketose *via* an Amadori rearrangement [1]. Recently, the lack of a *trpF* gene from the genomes of the actinomycetes *Streptomyces coelicolor* and *Mycobacterium tuberculosis* was experimentally clarified [2]. It was genetically demonstrated that these organisms contain a *hisA* homologue, annotated as *N*'-[(5'-phosphoribosyl)formimino]-5-aminoimidazole-4-carboxamide ribonucleotide (ProFAR) isomerase (HisA, EC 5.3.1.16), which is not only involved in histidine biosynthesis but also in the cognate isomerisation reaction catalysed by TrpF (Fig. 1). Thus,

these actinomycetes-specific *hisA* homologues were renamed *priA* (from *phosphoribosyl isomerases A*).

The evolution of the dual-substrate specificity of this unique ($\beta\alpha$)₈-isomerase has remained elusive; sequence analyses proved insufficient to identify relevant residues, which came as a surprise since the substrates PRA and ProFAR must impose significant functional constraints upon PriA, as they are different in size and in the total number of phosphoribosyl moieties that they contain (Fig. 1); moreover, the striking structural similarities between HisA and PriA [3] suggest that changes leading to the appearance of PriA dual-substrate specificity must be very subtle. Thus, it was clear that if the dual-substrate specificity of PriA was to be understood at the molecular level, the structure/function relationship of this enzyme ought to be established. With this aim in mind, we previously purified, crystallised and assayed the recombinant form of this enzyme for its TrpF activity [4] but unfortunately failed to solve the structure, until recently. Soon after this report

* Corresponding author. Fax: +52 777 3172388.

E-mail address: barona@ibt.unam.mx (F. Barona-Gómez).

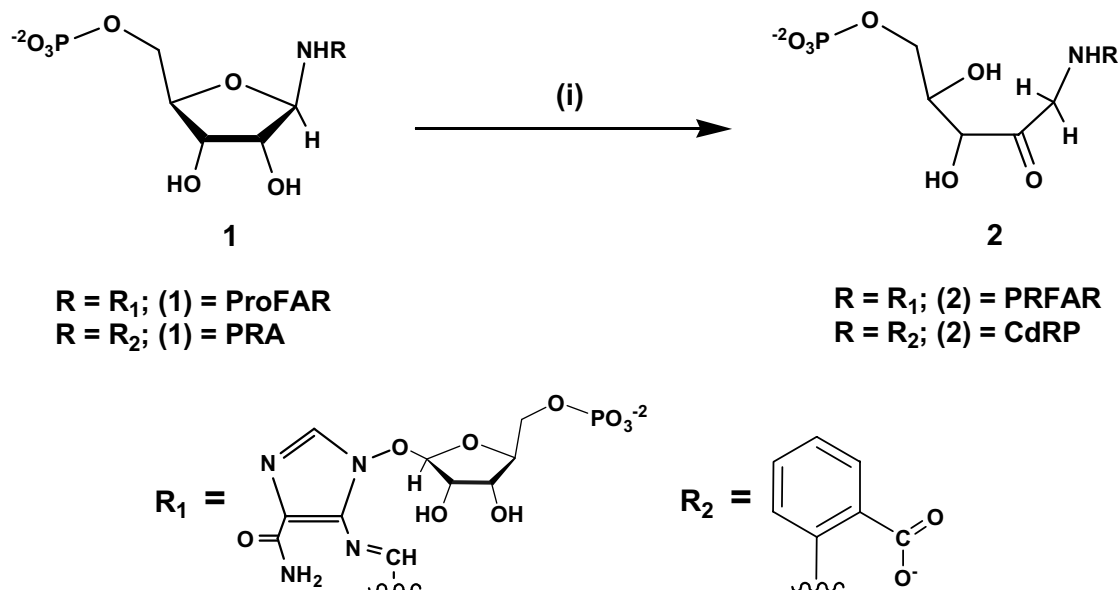


Fig. 1. Enzymatic reactions of PriA, HisA and TrpF. (i) PriA, HisA and TrpF catalyse Amadori rearrangements upon analogous phosphoribosyl substrates. PriA ($\text{R} = \text{R}_1$ or R_2), HisA ($\text{R} = \text{R}_1$) or TrpF ($\text{R} = \text{R}_2$). The products of ProFAR and PRA are *N'*-[(5'-phosphoribulosyl)formimino]-5-aminoimidazole-4-carboxamide ribonucleotide (PRFAR) and 1-[(2-carboxyphenyl)amino]-1-deoxyribose 5-phosphate (CdRP), respectively.

was published, a crystallographic structure of PriA of *S. coelicolor* at 1.8 Å resolution was published [3] showing that PriA adopts the anticipated $(\beta\alpha)_8$ -fold consisting of two symmetrical $(\beta\alpha)_4$ -halves. Unfortunately, some of PriA functional loops ($\beta \rightarrow \alpha$) lacked electron density in this structure (PDB: 1vzw), which undermined any rational mutagenesis experiments, leaving the structure/function relationship of this bifunctional enzyme undefined.

Here, we report the structural elucidation of two different conformers of PriA (1.8 Å) obtained under identical conditions, by means of the Multiwavelength Anomalous Dispersion (MAD) method. One of these structures is a closed conformer, which contains all of PriA loops. Notably, these findings have brought about novel structural insights including hitherto unnoticed molecular interactions, which were functionally characterised. We anticipate that the structure/function relationship of PriA established here will allow rational design of novel drugs targeting this enzyme present in *M. tuberculosis*. Moreover, these results may have a fundamental bearing on the evolution of the $(\beta\alpha)_8$ -fold as a whole, where co-occurrence of natural conformers and the link of these with the functional and structural versatility of the $(\beta\alpha)_8$ -barrels may become a recurring theme.

Materials and methods

Crystallisation, X-ray data collection, structure determination and refinement. Wild-type PriA and the mutant PriA_Ile⁶⁷Met, which was seleno-methionine (Se-Met) substituted, were purified and crystallised as previously reported [4]. For production of Se-Met substituted PriA, the methionine auxotrophic *Escherichia coli* strain B834(DE3) and M9 minimal medium were used [5]. Protein expression was induced with IPTG to 1 mM at an OD₆₀₀ of 0.6, and cell-growth was allowed to continue at 293 K for 16 h. 2-Mercaptoethanol was used at 2 mM in all buffers when

purifying the Se-Met substituted variant. Both native and Se-Met data sets were collected at the ESRF (Table S1, Supplementary Information). Data were processed using the HKL suite of programs [6]. The crystallographic phase problem was solved by SOLVE [7] using Se-edge MAD data and the resulting electron density map was interpreted by RESOLVE [8,9]. Refinement of the structures was carried out by alternate cycles of REFMAC [10] and manual refitting using O [11]. Water molecules were added to the atomic model automatically using ARP [12] at the positions of large positive peaks in the difference electron density, only at places where the resulting water molecule fell into an appropriate hydrogen-bonding environment. Restrained isotropic temperature factor refinements were carried out for each individual atom. The coordinates for wild-type PriA were deposited into the Protein Data Bank under the accession number 2vep.

Construction of PriA mutants. Single amino-acid mutations of PriA in pGEX-4T-1 were constructed using the megaprimer method [13]. The expression vector pET-PriASc [4] was mutated with a site directed mutagenesis kit (Stratagene) using standard conditions. All constructs were sequenced using vector universal primers prior to functional analyses.

Functional characterisation of PriA mutants. Complementation of *E. coli hisA* and *trpF* minus mutants was used for functional characterisation of mutated PriAs, since it has been shown that growth kinetics of *E. coli* mutants complemented with HisA and TrpF enzymes expressed in *trans* correlates well with enzyme kinetic parameters [1,14,15] allowing for a large number of mutant variants to be rapidly analysed. The histidine auxotroph used was HfrG6 *hisA* [16] and due to the uncharacterised requirement for Difco casamino acids of the available *trpF* mutant, i.e. W3110 *trpC* (Fdel), a *trpF* mutant (termed FBG-Wf) was constructed in a prototrophic background (JM101) using the lambda RED mutagenesis method (see Supplementary Information). Quantitative data from the complementation assays was obtained by growing the auxotrophic mutants bearing the pGEX-PriA constructs in LB broth with ampicillin (200 µg ml⁻¹) for 4 h, after which the cells were harvested by centrifugation (10 min, 1000g) and thoroughly washed three times. Twenty microlitres of pre-adjusted cell suspensions (1 × 10⁴ cells ml⁻¹) were used to inoculate in parallel LB-ampicillin and M9 plates. The pGEX-PriA derivatives were selected in M9 by their ability to rescue amino-acid auxotrophy, such that the ratio of the colony-forming units (CFUs) grown on LB over M9 plates could be established in terms of growth requirements. A decrease of ~10% CFUs on the M9 plate using wild-type PriA

was reproducibly recorded, and this ratio (~0.9) was normalised as 1 to quantitatively determine the effect of any given mutation. Growth time was recorded when colonies 0.1 mm in size could be detected.

Solubility assays or PriA mutants. Protein solubility assays *in vivo* were prepared using CoFi, which is a colony Western blot protocol that discriminates between soluble and insoluble proteins (see Supplementary Information). *In vitro* solubility assays were done using the same conditions and system as for expression and purification of wild-type PriA [4].

Results and discussion

Structure determination of a novel conformer of PriA

The Se-Met substituted (open conformer) and wild-type (closed conformer) structures of PriA are virtually identical, both in terms of their crystallographic parameters (Table S1, Supplementary Information) and the overall model they represent (0.32 Å rmsd for 199 common C α atoms). Ordering of different loops could in principle be related to the resolution at which each structure was refined, although both structures were elucidated at 1.8 Å resolution. The Se-Met derived model was refined against a near complete data set comprised of the first 30° of data collected at the beginning of the MAD experiment. There were no further features in

the electron density map observed from this refinement, leaving the same loops disordered as for the full dataset. Therefore, the observations discussed cannot be interpreted as a result of X-ray induced radiation damage; rather they are an intrinsic feature of the structures.

Since the crystallisation conditions used for wild-type PriA (PDB: 2vep) and Se-Met substituted PriA were identical, it can be concluded that these solved structures of PriA are crystallographically equivalent, implying natural co-occurrence of conformers. This conclusion is supported by the fact that the previously determined wild-type structure of PriA (PDB: 1vzw) elucidated at 1.8 Å resolution using virtually identical conditions, includes the same disordered loops [3]. Furthermore, superimposition of the structures reported here demonstrates that loops 1 and 6 undergo conformational changes: whereas the rmsd of the superimposed structures is only 0.32 Å, the distance between the last residues of loops 1 and 6 that appear well defined in the Se-Met structure, i.e. Gly²³ (loop 1) and Ala¹⁶⁹ (loop 6), is of 4.83 and 4.11 Å, respectively. Interestingly, these conformers co-occur irrespective of the presence of substrates since both structures have bound sulphate ions (Fig. 2).

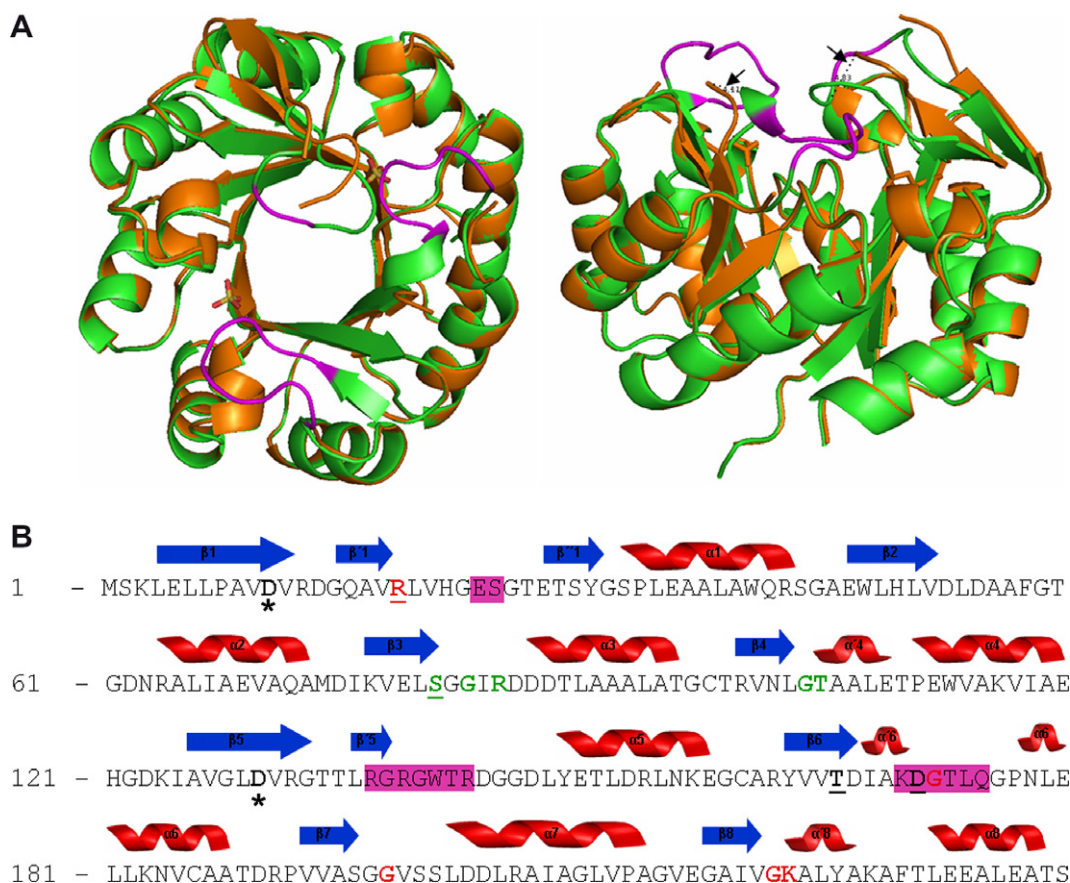


Fig. 2. Structural comparison of PriA conformers. (A) Bound sulphate ions (sulphur atoms in yellow) and the catalytic residues Asp¹¹ and Asp¹³⁰ are shown in a stick representation. The functional loops 1 and 6 in the closed conformer are coloured in magenta and the distance measured between residues Gly²³ (loop 1) and Ala¹⁶⁹ (loop 6) (4.83 and 4.11 Å, respectively) is shown with arrows (drawn with PyMOL). (B) Secondary structures and relevant residues of PriA are shown: Asp¹¹ and Asp¹³⁰ are marked with an asterisk; Thr¹⁶⁶ and Asp¹⁷¹ are underlined; N-terminal (green) and C-terminal (red) PBS residues, including Arg¹⁹ and Ser⁸¹, are also underlined. The regions that are missing from the open conformer are highlighted with magenta boxes. See text for further details. (For interpretation of the references to colour in this figure legend, the reader is referred to the web version of this article.)

The bifunctional active site of PriA

The functional and flexible loops 1 and 6 of wild-type PriA interact through a hydrogen bond formed by the backbone atoms of residues His²² and Asp¹⁷¹. Remarkably, these flexible loops, together with loop 5, which lacks some of the side-chains of its arginine residues (implying flexibility), follow β strands where residues presumed to be catalytically important for the HisA activity of PriA are present. These residues are Asp¹¹ (β 1), Asp¹³⁰ (β 5) and Thr¹⁶⁶ (β 6), which by analogy with HisA data [1,14,15] are presumed to be catalytically essential. As expected, mutation of Asp¹¹ and Asp¹³⁰ into alanine abolished both activities of PriA implying a direct catalytic role of these residues as either the general acid or the general base. These results were confirmed by protein solubility assays,

Table 1
Functional analysis of PriA mutant variants

Mutation	TrpF activity ^a	Time ^b (h)	HisA activity ^a	Time ^b (h)	Protein solubility ^c
Wild-type	1	31	1	40	+
Asp ¹¹ Ala	0	∞	0	∞	+
Arg ¹⁹ Ala	>1	31	0	∞	+
Ser ⁸¹ Thr	0	∞	0.93	71	+
Asp ¹³⁰ Ala	0.01	∞	0	∞	+
Asp ¹³⁰ Gln	0	∞	0	∞	+
Thr ¹⁶⁶ Ala	0	∞	0	∞	+
Asp ¹⁷¹ Ala	0.14	74	0	∞	+
(-) control	0	∞	0	∞	

^a The value reported (0–1) is a ratio of the total number of CFUs on LB over that on M9, and normalized against the data obtained for wild-type PriA, which equals 1. The mean value from at least three independent experiments is reported.

^b Time elapsed before appearance of visible colonies (0.1 mm in size); ∞ , did not complement.

^c The solubility of PriA mutants was determined both *in vivo* and *in vitro* (see Supplementary Figure S1).

showing that loss of the TrpF and HisA activities of these PriA mutants is unrelated to insolubility problems (Table 1 and Figure S1, Supplementary Information).

It was interesting to note, however, that the mutant variant PriA_{Asp¹³⁰Ala} occasionally showed very low levels of TrpF activity. The odd colonies that appeared were re-grown, their plasmids extracted, and re-sequenced to confirm the integrity of the constructs. This result is consistent with previous experiments with HisA [14,15] in which as a prerequisite for the TrpF activity of the mutant HisA_{Asp¹²⁷X}, the presence of an uncharged residue in this position was established. We therefore constructed the mutant PriA_{Asp¹³⁰Gln}, and in accordance with this observation, the TrpF activity of PriA was completely abolished (Table 1). Analogous to hydrolysis of bacterial peptidoglycans by lysozymes [17] one plausible mechanism for TrpF's activity of HisA_{Asp¹²⁷Val} and PriA_{Asp¹³⁰Ala} would be substrate-assisted acid catalysis involving the carboxylate of the anthranilate moiety.

Further light into the exact catalytic role of Asp¹¹ and Asp¹³⁰, was shed by ligand-docking simulations upon both structures using the products PRA and PRFAR. Coherent results could only be obtained using the closed conformer, implying that this may indeed be the catalytically relevant conformer of PriA. In agreement with previous data for HisA homologues [1,18] these simulations suggest that ProFAR is oriented such that the phosphoribosyl moiety that is attacked during catalysis interacts with the C-terminal phosphate-binding site (PBS). In contrast, only the N-terminal PBS appears to bind PRA (Fig. 3). Interestingly, the orientations encountered for PRA and ProFAR may imply that PriA may use Asp¹¹ and Asp¹³⁰ differentially as the general acid or the general base, depending upon which substrate is bound. The general base, which is responsible for abstracting a proton from the carbon atom next to the imine of the intermediary would be Asp¹¹ for the HisA activity (5.02 Å) and Asp¹³⁰ for the TrpF activity

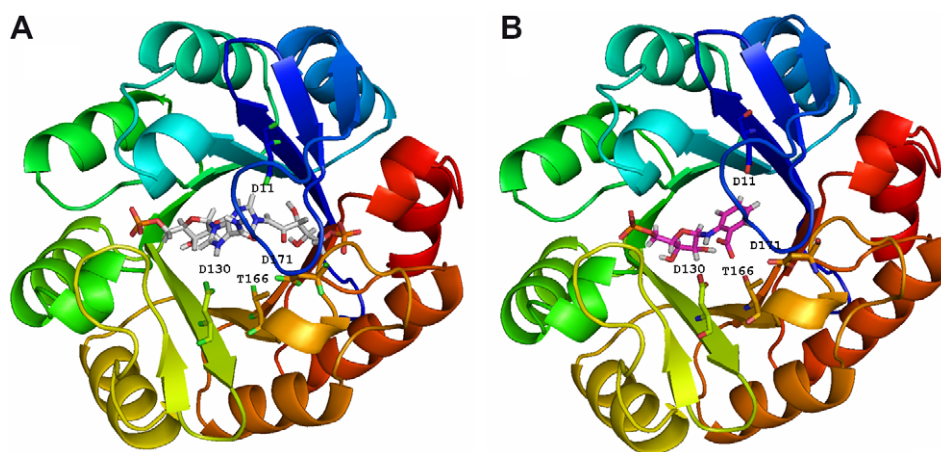


Fig. 3. The bifunctional active site of PriA. Ribbon diagram of the closed conformer of PriA coloured in blue (N-terminus) through to red (C-terminus) docked with PRFAR (A) and PRA (B). The ligand-docking simulations were done with Molegro Virtual Docker [20] using 3D coordinates of PRA obtained with PRODRG [21] and the reduced form of PRFAR (PDB: 1jvn). (For interpretation of the references to colour in this figure legend, the reader is referred to the web version of this article.)

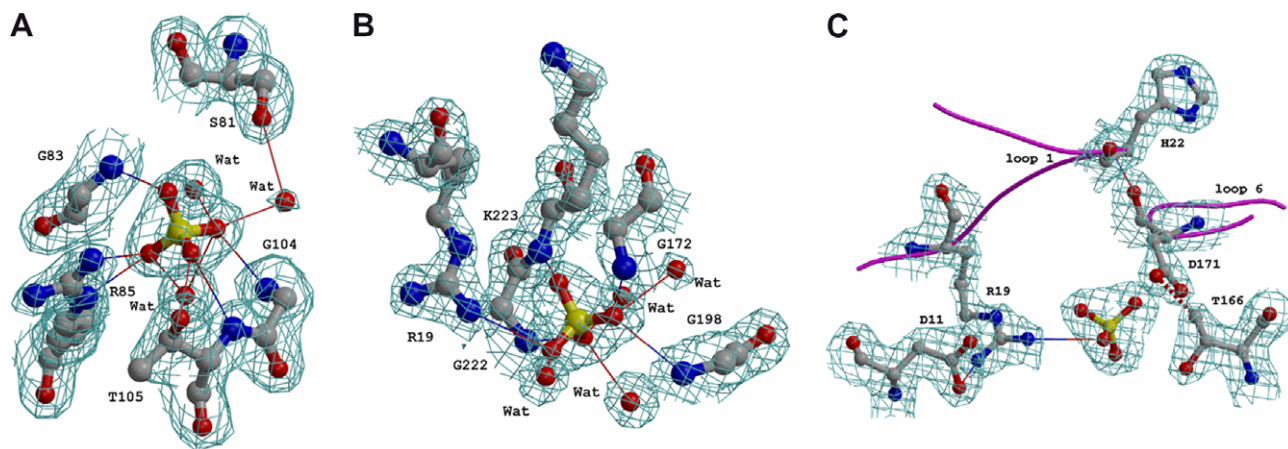


Fig. 4. Key molecular interactions of PriA. Hydrogen bonds are drawn as thin lines. The SIGMAA [22] weighted $2mF_o - \Delta F_c$ electron density using phases from the final model is contoured at 1σ level, where σ represents the rms electron density for the unit cell. Contours more than 1.4 \AA from any of the displayed atoms have been removed for clarity. (A) The N-terminal PBS, including Ser⁸¹. (B) The C-terminal PBS, including Arg¹⁹. (C) The unusual contact (2.57 \AA) between Thr¹⁶⁶ and Asp¹⁷¹ is shown as a red dotted line. Residue Asp¹³⁰ was omitted to allow proper visualisation, but if included, it would appear in front of Thr¹⁶⁶ and Asp¹⁷¹.

(4.85 \AA), and *vice versa* for the general acid. An interesting mechanistic implication of this proposal is that the bifunctionality of PriA may be regulated by the protonation state of these aspartate residues, which in turn may be mediated by subtle conformational changes.

The dual-substrate specificity of PriA

To experimentally validate the proposed specificities for PRA and ProFAR, the PBSs of PriA were scrutinised. Of the different residues participating in substrate recognition within either PBS, Ser⁸¹ (N-terminal) and Arg¹⁹ (C-terminal) were found to provide conclusive functional information. In *bona fide* bifunctional PriA homologues, the N-terminal PBS motif appears to be SGG, whereas in HisA monofunctional enzymes this motif is GGG (F.B.G., unpublished results). Although Ser⁸¹ is not directly interacting with the sulphate ion, it may potentially have a key role on substrate recognition since it forms a hydrogen bond with a molecule of water that contacts the sulphate ion (Fig. 4A). Motivated by this structural observation, we constructed the mutant PriA_Ser⁸¹Thr with the expectation that a longer side-chain could interfere with this recognition process. Interestingly, this mutation completely abolished the TrpF activity of PriA, but not its HisA activity, supporting the notion that only the N-terminal PBS binds PRA. This conclusion was supported by the fact that mutation of Arg¹⁹, which directly binds the sulphate ion with its side-chain (Fig. 4B), abolished exclusively the HisA activity.

A molecular switch for PriA conformational changes?

The equivalent residue of Thr¹⁶⁶ in HisA has been shown to be catalytically essential [1], although its exact role remains to be elucidated. As expected, mutation of this residue in PriA completely abolished both the HisA and

TrpF activities. This result was complemented with solubility assays making it unlikely that this double phenotype is due to protein solubility problems (Table 1 and Supplementary Figure S1). At a first glance, this would imply involvement of this residue during chemical catalysis *per se*. However, we could not find any sound structural evidence for Thr¹⁶⁶ acting as a catalytic residue (Fig. 3). In contrast, it should be noted that the structure of the HisA orthologue from *Saccharomyces cerevisiae*, termed His6, has been recently reported [18] showing that this residue is not conserved. Moreover, as it can be seen in the zoom-in of Fig. 4C the side-chain methyl group of Thr¹⁶⁶ is making a short contact (2.57 \AA) with the carboxylate of Asp¹⁷¹, which is also involved in closing the active site together with His²². Short C–H...O hydrogen bonds are relatively rare, but have been seen before [19]. The electron density and the corresponding model are well defined at this region and therefore this observation cannot be regarded as an artefact. Based on this observation, it is tempting to speculate that this unusual contact is acting as a molecular switch that may mediate between the two naturally co-occurring conformers of PriA. In support of this, mutation of Asp¹⁷¹, which is unlikely to have a catalytic role, abolished the HisA activity completely, and the TrpF activity was decreased by tenfold. Interestingly, this unusual contact is absent from any of the HisA structures that have been so far solved, despite the fact that these residues are 100% conserved.

Acknowledgments

This work was funded by CONACyT, Mexico (Project No. 50952-Q) and the Royal Society, UK (Project No. 20060612184333-3475-43146). We are grateful to Filiberto Sánchez, Paul Gaytan and Jorge Yañez for technical assistance and the European Synchrotron Radiation Facility (ESRF) for access and user support.

Appendix A. Supplementary data

Supplementary data associated with this article can be found, in the online version, at [doi:10.1016/j.bbrc.2007.10.101](https://doi.org/10.1016/j.bbrc.2007.10.101).

References

- [1] M. Henn-Sax, R. Thoma, S. Schmidt, M. Hennig, K. Kirschner, R. Sterner, Two $(\beta/\alpha)_8$ -barrel enzymes of histidine and tryptophan biosynthesis have similar reaction mechanisms and common strategies for protecting their labile substrates, *Biochemistry* 41 (2002) 12032–12042.
- [2] F. Barona-Gómez, D.A. Hodgson, Occurrence of a putative ancient-like isomerase involved in histidine and tryptophan biosynthesis, *EMBO Rep.* 4 (2003) 296–300.
- [3] J. Küper, C. Doenges, M. Wilmanns, Two-fold repeated $(\beta\alpha)_4$ half barrels may provide a molecular tool for dual substrate specificity, *EMBO Rep.* 6 (2005) 134–139.
- [4] H. Wright, F. Barona-Gómez, D.A. Hodgson, V. Fülöp, Expression, purification and preliminary crystallographic analysis of phosphoribosyl isomerase (PriA) from *Streptomyces coelicolor*, *Acta Crystallogr. D, Biol. Crystallogr.* 60 (2004) 534–536.
- [5] W.A. Hendrickson, J.R. Horton, D.M. LeMaster, Selenomethionyl proteins produced for analysis by multiwavelength anomalous diffraction (MAD): a vehicle for direct determination of three-dimensional structure, *EMBO J.* 9 (1990) 1665–1672.
- [6] Z. Otwinowski, W. Minor, Processing of X-ray diffraction data collected in oscillation mode, *Macromolecular Crystallography. Pt. A*, 276, Academic Press Inc., San Diego, 1997, pp. 307–326.
- [7] T.C. Terwilliger, J. Berendzen, Automated MAD and MIR structure solution, *Acta Crystallogr. D, Biol. Crystallogr.* 55 (1999) 849–861.
- [8] T.C. Terwilliger, Maximum likelihood density modification, *Acta Crystallogr. D, Biol. Crystallogr.* 56 (2000) 965–972.
- [9] T.C. Terwilliger, Automated main-chain model-building by template-matching and iterative fragment extension, *Acta Crystallogr. D, Biol. Crystallogr.* 59 (2003) 38–44.
- [10] G.N. Murshudov, A.A. Vagin, E.J. Dodson, Refinement of macromolecular structures by the maximum-likelihood method, *Acta Crystallogr. D, Biol. Crystallogr.* 53 (1997) 240–255.
- [11] T.A. Jones, J.Y. Zou, S.W. Cowan, M. Kjeldgaard, Improved methods for building protein models in electron density maps and the location of errors in these models, *Acta Crystallogr. A* 4 (1991) 110–119.
- [12] A. Perrakis, T.K. Sixma, K.S. Wilson, V.S. Lamzin, wARP: improvement and extension of crystallographic phases by weighted averaging of multiple-refined dummy atomic models, *Acta Crystallogr. D, Biol. Crystallogr.* 53 (1997) 448–455.
- [13] M. Kammann, J. Laufs, J. Schell, B. Gronenborn, Rapid insertional mutagenesis of DNA by polymerase chain reaction (PCR), *Nucleic Acids Res.* 17 (1989) 5404.
- [14] C. Jürgens, A. Strom, D. Wegener, S. Hettwer, M. Wilmanns, R. Sterner, Directed evolution of a $(\beta/\alpha)_8$ -barrel enzyme to catalyze related reactions in two different metabolic pathways, *Proc. Natl. Acad. Sci. USA* 97 (2000) 9925–9930.
- [15] S. Leopoldseder, J. Claren, C. Jürgens, R. Sterner, Interconverting the catalytic activities of $(\beta\alpha)_8$ -barrel enzymes from different metabolic pathways: sequence requirements and molecular analysis, *J. Mol. Biol.* 337 (2004) 871–879.
- [16] T.S. Matney, E.P. Goldschmidt, N.S. Erwin, R.A. Scroggs, A preliminary map of genomic sites for F-attachment in *Escherichia coli* K12, *Biochem. Biophys. Res. Commun.* 17 (1964) 278–281.
- [17] I. Matsumura, J.F. Kirsch, Is aspartate 52 essential for catalysis by chicken egg white lysozyme? The role of natural substrate-assisted hydrolysis, *Biochemistry* 35 (1996) 1881–1889.
- [18] S. Quevillon-Cheruel, N. Leulliot, M. Graille, K. Blondeau, J. Janin, H. van Tilbeurgh, Crystal structure of the yeast His6 enzyme suggests a reaction mechanism, *Protein Sci.* 15 (2006) 1516–1521.
- [19] Z.S. Derewenda, L. Lee, U. Derewenda, The occurrence of C–H...O hydrogen bonds in proteins, *J. Mol. Biol.* 252 (1995) 248–262.
- [20] R. Thomsen, M.H. Christensen, MolDock: a new technique for high-accuracy molecular docking, *J. Med. Chem.* 49 (2005) 3315–3321.
- [21] A.W. Schuettelkopf, D.M.F. van Aalten, PRODRG—a tool for high-throughput crystallography of protein–ligand complexes, *Acta Crystallogr. D* 60 (2004) 1355–1363.
- [22] R.J. Read, Improved Fourier coefficients for maps using phases from partial structures with errors, *Acta Crystallogr. A* 42 (1986) 140–149.